Romanian Journal of Ecology & Environmental Chemistry, 4(2), 2022
https://doi.org/10.21698/rjeec.2022.206

Review

Short review on mechanical activation in non-metallurgical alumina production

LIDIA KIM[1], GHEORGHE DOBRA[2], RALUCA ISOPESCU[3], SORIN ILIEV[4], LUCIAN COTET[4], ALINA BOIANGIU[4], LAURENTIU FILIPESCU[3]

[1]*National Research and Development Institute for Industrial Ecology - ECOIND, 57-73 Drumul Podu Dambovitei Street, 060652, Bucharest, Romania*
[2]*Alro SA, 116 Pitesti Street, Slatina, Romania*
3Polytechnic University of Bucharest, Faculty of Chemical Engineering and Biotechnology, 7 Polizu Street, Bucharest, Romania
[4]*Alum SA, 82 Isaccei Street, 820228, Tulcea, Romania*
** Corresponding author: lidia.kim@incdecoind.ro*

Received:	*Accepted:*	*Published:*
14.12.2022	*20.12.2022*	*28.12.2022*

Abstract
The terms mechano-chemistry and mechanical activation of solid materials were introduced in chemical literature by Ostwald at the beginning of the XX century. Both terms cover a whole range of interconnected phenomena taking place during the mechanical action on solids or their separate parts participating in chemical reactions, phase transitions, mixing and creating composite materials, alloying and crystal growth in the solid state, deformation and changing physical and thermal properties, all of them at low temperature. The common effects of the mechanical activation on solid material are fracturing and reduction of particle sizes, generation of new reactive surfaces, diffusion of atoms of the reactant phase through the product phase, and quite significantly, accumulating energy in crystalline or amorphous structure (enough twists in atomic and molecular networks, tensions in atomic bond and active sites to trigger the nucleation of new phases). Mechanical activation is very used to produce all clean alumina mineralogical phases with uniform particle size dimensions from nano to macro size. Also, mechanical activation may extend the specific surface of some minerals, enhancing the yields in the solid-liquid extraction process. With adequate precursors, all phase transitions from amorphous to alfa α-Al_2O_3 can be carried out on the same route as in thermally activated alumina, but some other routes, impossible by thermal activation, might be followed. The difference between the two activation ways is that mechanical activation is made at room temperature.

Keywords: *non-metallurgical alumina, mechanical activation, boehmite, Gibbsite, low-temperature*

INTRODUCTION

Mechanical activation is a part of mechano-chemistry, the fundamental science that supports a wide range of potential applications. Mechanical activation itself is largely an innovative technology, that, primarily, concerned combinations between the new surface expansion or controlled shrinkage, and also, defect formation on crystalline surfaces. In many of mechanical activation technologies, the main target is the rationale use and saving the energy consumptions. Mechanical activation is of uncommon importance in the mineral processing, also in chemical engineering, extractive metallurgy, waste disposal and recovery, environmental chemistry and other new special area, like medicine nano-materials synthesis and synthesis of chemical compounds.

The purpose of this review is to discuss the topics related to mechanical activation technology applied in the field of non-metallurgical alumina. However, the abundance of works covering this field is overwhelming. Thus, information carried by this review will be limited to low temperature non-metallurgical alumina in last two decade of 21th century.

Aluminum hydroxide, as an intermediary wet product (gibbsite, $Al_2O_3 \cdot 3H_2O$), is industrially produced by Bayer process from different kinds of bauxites. The gibbsite quality, particle size, crystallinity and crystals morphology are strongly influenced by the Bayer process parameters [1-6].

Parts of the gibbsite production are converted by calcination into alumina for metallurgical use and for high temperature ceramic alumina. The rest of production undergo large chemical and thermal treatments, size dimensions classification, as well as other required finishing operations for being used in the wide-ranging new high technology applications.
Aluminum hydroxide and its related products highly required on the market are very important materials with various industrial applications, mainly as: filers and fire retardants [7-19], desiccants [20-26], adsorbents and water purification reactants [27-37], coating materials [38-47], composite materials [48-56], catalysts and catalyst support [57-66], environmental alumina [66-67] and synthesis of chemical compounds [67-69].

Characterization of the non-metallurgical alumina

Clasification of non-metalurgical aluminas

Primary hydrates are raw aluminum hydroxide product types from Bayer technology, available in wet and dry states. These products serve as materials for producing metallurgical alumina (85-90%) and for manufacturing non-metallurgical alumina products (10-15 %). The variety of non-metallurgical alumina products is vast and increases annually in the number of products and new applications.
Dry or wet crude hydrate of varying purity is used as a raw material for manufacturing aluminum sulfate and aluminum poly-chlorides, aluminum fluoride, cryolite, and zeolites, as well as purified sodium aluminate as a raw material for the manufacture of other fine chemicals with multiple applications and guaranteed profitability.
Special hydrates are varieties of aluminum hydroxide obtained by precipitation from purified sodium aluminate or resulting from the redissolution of the crude hydrate in the pure sodium hydroxide. These products are used to manufacture flame retardant fillers, adsorbents, desiccants, ceramic and high-temperature materials, catalysts, catalyst supports, and other industrial materials.
Activated alumina are aluminum oxyhydroxides resulting from the thermal, hydrothermal, and chemical dihydroxylation of hydrates, with various degrees of purity, coming from Bayer alumina technology.
Calcined oxides with refractory properties are obtained from primary hydrates (with various degrees of purity), dried, and classified. These products are raw materials for manufacturing tabular alumina, cements with tricalcium aluminate content, fused alumina, and other refractory materials with low mixes oxide content.
Calcined oxides for obtaining non-refractory materials come from various types of calcined alumina and serve to manufacture ceramics for fused alumina and abrasive materials.

Commercial types of alumina products

Smelter grade alumina (SGA) is used as raw material in the electrolytic manufacture of aluminum. For the production of the SGA, alumina hydrate (gibbsite) is completely dehydroxylated in flash calciners. At 600ºC, most of the water is evaporated, and the products are various types of activated alumina containing predominantly γ-alumina and some amorphous and transition phases. Around 800-850ºC, the product is crystalline γ-alumina with a surface area of around 50 m^2/g. At temperatures higher than 1000ºC, the recrystallization of α-alumina begins [70,71].
The calcined alumina products are obtained at temperatures higher than 1100ºC when the main recrystallized mineralogical phase is α-alumina. Various mineralizers are added to the raw gibbsite to lower the recrystallization temperature of α-alumina. These alumina products are used in various ceramic and refractory applications [72-74].
Low Soda Alumina. Many applications, particularly in the electrical/electronic industrial areas, require a low level of soda to be present in the alumina. Low soda alumina is generally defined as an alumina hydrate with soda content of less than 0.1% by weight. This can be manufactured by many different routes, including acid washing, chlorine addition, boron addition, and the use of soda adsorbing compounds [75-77].

"Reactive" alumina is the term generally given to a relatively high purity with small crystal size (<1 μm) alumina type, which sinters to a fully dense body at lower temperatures than low-soda, medium-soda or ordinary-soda alumina. These products are normally sold as powders after intensive ball-milling, breaking up the particulate material from thermal treatments [78-80].
Tabular alumina is produced by pelletizing, extruding, or pressing calcined alumina into shapes and then heating these shapes to a temperature just under their fusion point, 1700-1850ºC in the shaft kilns. The shaped material may be braked up, screened, and ground to produce the required range of sizes. Because the material was sintered and has especially low porosity, high density, low permeability, good chemical inertness, and high refractoriness, it could be used in refractory applications [81, 82].
The fused alumina has a high density, low porosity, low permeability, and high refractoriness. As a result of these characteristics, it is used in the manufacture of abrasives and refractories. Such products are manufactured in electric arc furnaces at a temperature close to the alumina melting point in batches of 3-30 tones [83, 84].
High-purity alumina is classified as a material with a purity of 99.99%. These high-purity products are manufactured by routes starting from Bayer hydrate, using successive activations and washings or via aluminum chloride to achieve the necessary degree of purity [85-88].

Short analysis of the non-metallurgical alumina production and market
Bauxite is the primary source of alumina both for obtaining metallurgical quality alumina and for non-metallurgical quality alumina. Metallurgical alumina is used for aluminum production, and non-metallurgical alumina is used in a wide range of industrial applications reviewed in this paper. The total world production of bauxite is about 300 m tpy, but it is estimated that only 10-15 m tpy are generally used for non-metallurgical applications. Of the total amount of bauxite extracted, approximately 80-85% is processed by the Bayer alumina process to obtain alumina trihydrate (ATH) and, further, by calcination, smelting alumina (SGA) to obtain electrolytic aluminum. The amount of raw bauxite left over from these processes is used to produce non-metallurgical bauxite of various grades (refractory, abrasive bauxite, high aluminum cement, activated bauxite, alumina-based ceramic support agents, etc.). Non-metallurgical bauxite can be classified into three main classes: abrasive-grade bauxite used to produce abrasive materials; chemical-grade bauxite, used to make aluminum chemicals; and refractory-grade bauxite, used to produce high-alumina refractories. Approximately 1.2 million tpy of calcined bauxite is used for refractories materials, with a small amount used for abrasive materials. Alumina trihydrate (ARH) is using to produces non-metallurgical alumina of various grades, such as aluminum chemicals, low-soda alumina, and activated alumina, including fillers and pigments for plastics and elastomers, special calcined alumina for ceramics, soft and burnt alumina for alumina cement, calcium aluminate cement and mineral wool. Other uses include aluminum fluoride and zeolites [89].
The non-metallurgical grade alumina available on the market is estimated at 8 million tpy and is also known as chemical grade alumina. From this alumina, approximately 60% is used to manufacture aluminum sulfate for water treatment, while fine alumina is used as a fire retardant. Brown fused alumina (BFA) is an abrasive mineral widely used in various applications. Calcined bauxite containing small concentrations of iron and other impurities is used together with BFA (approximately 40-50%) to obtain refractory materials. Of the refractory materials containing bauxite, approximately 70% are used in the steel industry, the rest being used in the glass industry and cement kilns. Calcined alumina is also used with alumina hydrate to obtain alumina chemical substances.
Table 1 shows the distribution of non-metallurgical bauxite in various applications. The vast majority of non-metallurgical bauxite used to obtain non-metallurgical alumina is found in China, either domestically produced or imported from Guyana. [89].
The leading non-metallurgical bauxite producers in 2022 are China, Germany, France, India, Turkey, Brazil, and Greece. The leading non-metallurgical alumina consumers in 2022 are found in France, Germany, the US, China, Brazil, and Sweden, according to USGS, the International

Committee for Study of Bauxite, Alumina, and Aluminum (ICSOBA), International Aluminum Institute (IAI), and other industry sources, as FastReport 2022 [89].

Table 1. Bauxite applications by market [89]

Application	Consumption (tpy)	Consumption (%)
Portland cement	2 m	18%
Refractories	1.2 m	11%
Abrasives	1.2 m	11%
Iron and steel slags	800,000	7%
Chemicals	800,000	7%
Calcium aluminate cement	450,000	4%
Proppants	200,000	2%
Mineral wool	200,000	2%
Welding	60,000	>1%
Anti-skid road surfacing	10,000	>1%
Other	4 m	37%

Mechanical activation technology

Mechano-chemistry is a relatively new chapter in the approach of chemical reactions involving solid phases with complex mineralogy. The mechanical activation is related to the degree of the solid phase comminution, the stress of the particles during compression, shearing, and braking, as well as the speed with which the mechanical energy is transferred to each individual particle [90-92]. Mechanical activation involves reactions in the solid phase, phase transformations, stress and deformation, structural defects, local thermal effects, bridges between the crystals, and fractures of the newly formed crystals and aggregates, which create new reactive surfaces. Materials humidity promotes chemical reactions, phase transformations, stress and deformation, structural defects, local thermal effects, bridges between the crystals, and fractures of the newly formed crystals, which create new reaction surfaces. Also, water occurrence at the surface of the particle produces polarization of the surfaces by adding OH^- ions, change in properties of the electric double layer on the particles surface, and surface transport of the dissolved material. To better understand the alumina phase transformations induced by mechanical activation in the non-metallurgical alumina process, the phase diagram from Figure 1 is highly required [93].

Mainly, the changes induced by the mechanical activation process are: a) grinding up to dimensions of the order of microns; b) generation of new contact surfaces and their expansion; c) formation of major dislocations and defects in the crystalline structure of materials, including the reduction of crystallite sizes; d) phase transformations in the polymorphic materials; e) chemical reactions such as decomposition, hydration, formation of complexes and adducts, the oxidation, reduction and alloying, and in the last instance, the cold reactions between reactive compounds, only at high temperature [93].

Recently, some reviews indicated that mechanical activation might be classified as a one-stage or two-stage process [94-98]. The one-stage mechano-chemical synthesis process is usually leaded with high-energy mills, where reactive particles are milled and activated. As a result, the chemical transformations of the initial reagents are taking place due to the formation of the new interfacial surface and the accumulation of additional energy in the system. Thus, the final reaction product recrystallization is consequentially accelerated. In the case of two-stage mechano-chemical synthesis, the first stage mainly comprises the grinding and preliminary mechanical activation of the powder mixtures up to an intermediary pre-activated reactive state, while in the second stage, the pre-activated product is converted into a final product with another or without the assistance of any mechanical activator. As a rule, the synthesis of a mechanically pre-activated mixture is characterized by high rates of physical or chemical transformations. One particular priority is controlling the temperature in both stages of the activation process. If not, unpredictable developments may arise in the overheated system, involving melting, sintering, and agglomeration

of the entire material. In addition, during continuous phase transitions, the accumulated excess energy might be lost by structural normalization of the components undergoing a critical phase transition [94-98].

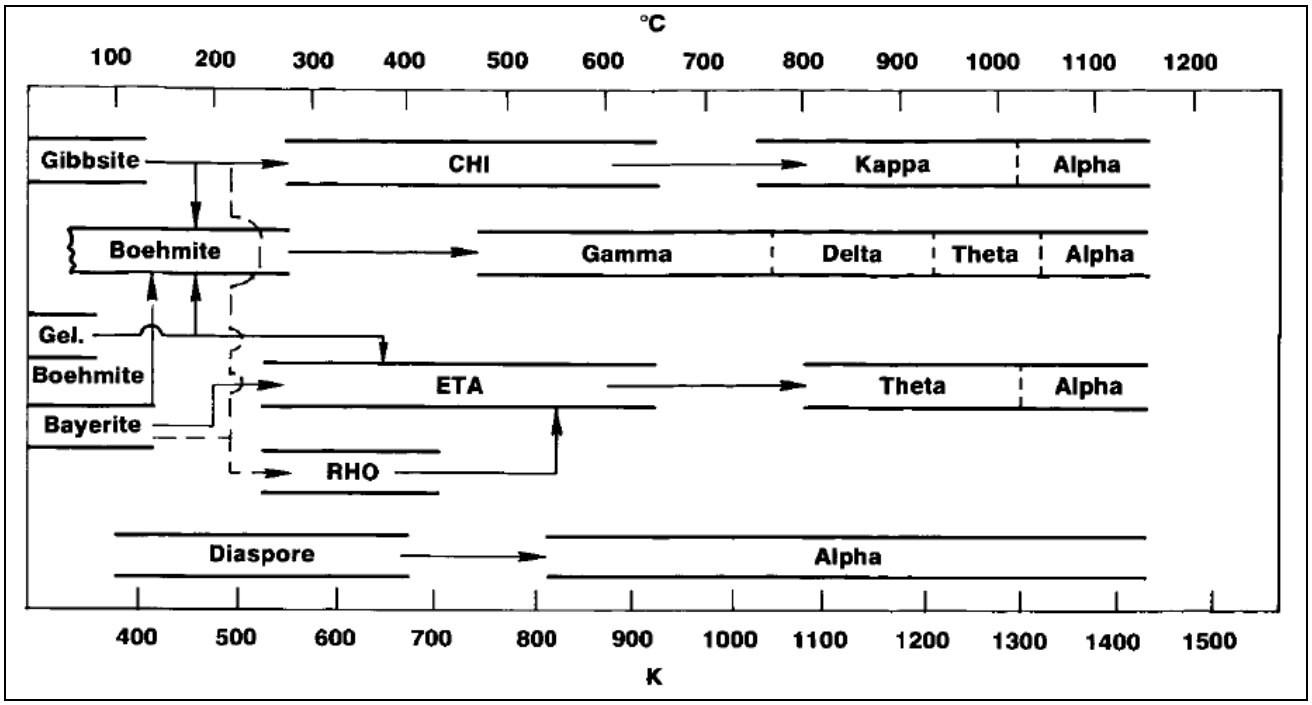

Fig. 1. Phase transitions of alumina mineralogical phases [93]

The objectives of coarse and fine grinding are to dislodge the associated mineral phases, to reduce the average particle size, associated with enlargement of the specific surface area of the particles and to accelerate chemical reactions. In principle, coarse grinding is a first phase of mechanical activation, but there are consumers who are interested in this type of grinding.
The objectives of mechanical activation aimed at structural changes of the mineralogical phases in activated material, as a result of the mechanical energy applied to the particles surface. Mechanical activation is applied in the following industrial fields: mechanical alloying, preparation of ores, leaching of ores and extractive metallurgy, sintering of materials, manufacture of pigments and paints, manufacture of pharmaceutical and geopolymers products to which new areas of application are constantly being added. [99-103].

Gibbsite mechanical activation - gibbsite to α-Al_2O_3
Gibbsite is the dominant phase in many types of bauxite used to obtain alumina for metallurgical and non-metallurgical use. For this reason, the deep understanding of the mechanical activation of this mineralogical phase is important for the industrial processing of all the raw materials that contain it. Also, it is equally important to study the transformation processes through mechanical activation of gibbsite into other more valuable polymorphic phases with wide-ranging applications in the industry of fillers and flame retardants, desiccants, absorbents and catalysts, varnishes and paints, abrasive materials, fine ceramics and high-temperature alumina, cosmetics and medicine, and especially, in the electronic industry.
The activation of gibbsite with a ball attrition mill led to significant results under the following experimental conditions (temperature: 25 ºC; sample mass: 100 g; ratio solid/ liquid: 1/2; ball/gibbsite ratio: 20/1; balls diameter: 2 mm; grinding time: 0-30 minutes; stirring speed: 1000 rpm). Thus, the median size of the distribution moved from 52 μm to 3 μm after an activation time of 30 minutes. The same grinding procedure was applied to gibbsite-hematite and gibbsite-quartz mixtures, with similar results. The activated samples were characterized by granulometry measurements, X-ray diffraction, SEM microscopy, zeta potential, and isotonic point. The

summarized results are: the median size of the particles is of the order 3 μm, the distribution of the particle sizes quickly passes from a unimodal distribution to a bimodal distribution (as proof of the breaking of particles during activation), the morphology of the activated product passes from the known morphology of agglomerates, formed by disc-shaped units, to a complete altered morphology, by particles fragmentation [104, 105]. The XRD studies have proven that the product obtained is mostly amorphized. The authors confirmed the older observations regarding the existence of a well-defined correlation between the grinding rate of the gibbsite and the impact energy of balls [106]. The latter works of the same authors, regarding the mechanical activation of gibbsite in two mills with significant constructive differences in operating principles, showed that attrition mills are superior to planetary mills since they induce a greater reactivity to the activated gibbsite than planetary mills under the identical conditions from the experimental point of view [107, 108].

Another sequence of phase transformations occurs when mechanical activation is performed in the absence of air. At room temperature, the monoclinic gibbsite $Al(OH)_3$, mechanically activated in a nitrogen stream, was converted into nano-crystalline orthorhombic boehmite (γ-AlOOH). The boehmite phase forms slowly and becomes reactive after 3 hours of mechanical activation when the boehmite begins to increase quantitatively at a noticeable speed. After 40 hours of mechanical activation, almost the entire amount of gibbsite transforms into nanocrystalline boehmite along with small alpha-alumina crystallites with a size of 2-3 nm. When calcined in a fluidized bed with an air heating rate of 10°C/min, the nanocrystalline boehmite transforms into gamma alumina at 520°C and then, into alpha-alumina at 1100ºC, having the crystal size of 100-200 nm. After the thermal activation of boehmite, the sequence of phase transformation gibbsite - boehmite at 220°–330°C is inactivated and alpha-alumina appered at 1100°C. This is an unexpected route, but alfa-alumina is accompanied by the formation of δ-Al_2O_3 and θ-Al_2O_3 as the transitional phases, as usually happens with inactivated boehmite phase. The resulting powder consists mostly of agglomerated particles with a size of 0.4-0.8 μm [109].

Jang et al. [110] observed that the industrial gibbsite, without any preliminary treatment, in a Fritsch Pulverisette 7 mill, was amorphized proportionally with the length of activation time, up to a degree of amorphization of 90-95% at normal temperature. Upon isothermal heating, after mechanical activation, the gibbsite transforms into alpha-alumina at 850-900ºC, while, in the case of non-activated alumina, this transition occurs at 1050-1100ºC. The XRD analyses on the same samples, performed around the temperatures mentioned above, showed that in the mechanically activated samples, the transitional phases κ-Al_2O_3 and χ-Al_2O_3 appeared before the total conversion into α-alumina (according to the normal transition route of pure gibbsite). However, in the case of mechanically non-activated samples, the transitional phases formed are δ-Al_2O_3 and θ-Al_2O_3, probably as the difference between the precursors in amorphous gibbsite and, respectively, precursors in hydrated alumina. In conclusion, the amorphous alumina synthesized after mechanical activation did find out its transition precursors to alfa α-alumina to lower temperature, about 850-950 ºC.

Karagedov [111, 112] studied the seeding with α-alumina all the available precursors to be transformed into α-alumina by mechanical activation and proposed a method of obtaining α-alumina from pure chemical reagents: aluminum nitrate and ammonia, and respectively, Bayer gibbsite. This method has 3 experimental stages: a) the precipitation of colloidal gibbsite through the reaction of aluminum nitrate with ammonia and the formation of the gel at 70 ºC, which serves as a primer for the formation of α-alumina; b) synthesis of the precursor by mixing the gel with gibbsite in proportions of 3-10% gel, calcining the material at 800-930ºC, and c) light grinding to obtain alpha-alumina powders. The first stage is similar to the preparation of alumina nanoparticles, which usually form a gel, then calcined at a suitable temperature to obtain alpha-alumina [111, 112]. In the second stage, the alpha-alumina formation reactions in the previously prepared gel take place in the gibbsite particles mass, and the alpha α-alumina particles from the gel serve as precursors for initiating the gibbsite transformations by several transitions to alpha-alumina, at any temperature, inside the interval mentioned above. Depending on the amount and method of

introducing the seeding agent, the complete transformation of the precursors to α-Al_2O_3 occurs at a temperature between 800 and 930 °C. In this stage, aggregate particles with dimensions of 10-20 mm are formed, having variable shapes and significant porosity. A light grinding of these aggregates leads, in stage 3 of the process, to an alpha-alumina powder with a typical particle diameter of 50-60 nm [111].

MacKenzie et al. [113] have another view on the above transition routes. Gibbsite was mechanically activated by grinding for 20 h, and the changes in its structure were studied by thermal analysis, X-ray powder diffraction, and MAS NMR. The activated material has lost significant proportions of the Al–OH bonds, but the resulting molecular water was immediately adsorbed onto the activated surfaces. Also, this water could be desorbed at 125°C (endothermic effect). However, the only notable change observed after activation was the amorphous state of the entire sample. In this experiment, the authors have found that coordination related to site occupancies suggests that this phase is similar to rho ρ-Al_2O_3. However, the amorphous phase follows transition via γ-Al_2O_3 to α-Al_2O_3 (corundum) at 900°C, while the non-activated gibbsite exhibits transitions to corundum via γ-Al_2O_3 and θ-Al_2O_3 at a temperature of about 400°C [113].

Tsuchida and Ichikawa [114] studied the mechanical activation of gibbsite, bayerite, and boehmite. They made comparisons of the evolution of these phases during activation regarding texture, structure, and thermal behaviour, using the laboratory equipment: XRD, TG, DTA, SEM, IR, particle size distribution, and nitrogen adsorption (surface and pores studies). The samples were ground at normal temperatures for between 0.25 and 20 hours using a planetary-type ball mill. The measurements showed that, in the initial stages (activation under 60 minutes), the specific surface increased for gibbsite, decreased for bayerite, and had the maximum value for boehmite.

These variations in specific surface area were correlated with the average particle size representing aggregates or individual particles. It was also noticed that the diffraction lines of the three materials decreased in intensity, and after 4-8 hours of grinding, the three materials dehydrated and amorphized.

The DTA data show that an endothermic transformation occurs between 150 and 200 °C due to the recrystallization of a good part of the material. During recrystallization, phase transitions occur in the 25-200°C range. The phase transformations are different for all 3 samples as follows:

gibbsite → χ → κ → α (1)

gibbsite → χ → κ → α (2)

boehmite → γ → δ → θ → α (3)

gibbsite amorphous → η → α (4)

As could be seen, alpha-alumina appears in activated gibbsite samples even at low temperatures above 200°C [114, 115].

Mechanical activation of boehmite - boehmite to α-Al_2O_3

The mechanical activation of boehmite was studied by a large group of researchers [104, 105, 116-120], with the aim of analyzing and explaining the nature of the changes in the crystalline structure of mechanically activated boehmite, firstly for lowering the boehmite transformation point into α-alumina, and secondly for increasing reactivity of activated product in the reaction with sodium hydroxide, when the bauxites with high boehmite content are used as raw materials in Bayer's alumina manufacturing technology.

The studies were carried out on boehmite crystallized in hydrothermal conditions or on boehmite prepared by decomposing gibbsite (coarse crystals with size d50 =120 μm) in the air at 350°C for 2 hours in a static furnace.

The pure product was characterized by TG/DTA and XRD studies, confirming the synthetic boehmite's crystallinity. The study of the morphology of boehmite, resulting from the thermal decomposition of the gibbsite, shows that the particles are uniform and preserve the structure of the gibbsite agglomerates. The slit-shaped pores come from the process of preferential evaporation of water from the interlamellar space of the crystallographic structure.

Karagedov and Lyakhov [120] identified in the milling process four distinct stages: coarse milling, breaking the larger particles (first stage), followed by fine grinding, which contributed to the decrease of the particle size and promoting aggregation of the smallest particles (second stage) and further densification of the aggregates (third stage), accompanied by amorphization of new phase particles (fourth stage). The mechanical activation of synthetic boehmite was done in batches in a planetary ball mill (Pulverisette P6, Fritsch GmbH, Germany) at normal temperature. The boehmite sample had a mass of 30 grams, the ball/sample mass ratio was 10/1, and the mill rotation speed was 400 rpm. The rotation direction was changed every 5 minutes, and the grinding time was set between 0 and 240 minutes. The measured characteristics of the mechanically activated sample were: particle size distribution (Size analyzer Model: Mastersizer, Malvern, U.K.), BET specific surface area with nitrogen adsorption (Surface area analyzer Micromeritics (USA, Model: ASAP2020), particle morphology (SEM microscope, Model: 840A JEOL, Japan). The degree of amorphization of boehmite, the size of the micro-crystallites, and the elastic deformation of the crystal lattice were calculated from X-ray diffraction (XRD) data (Siemens diffractometer Model: D500), and the chemical structure from FTIR data (Spectrometer Nicolet 5700). The reactivity of the activated samples was evaluated from measurements of the amorphous boehmite → α-Al_2O_3 phase transformation temperature (TG–DTA, model: SDT Q600, TA Instruments, USA) and measurements of the leaching yield of standard bauxite with alkaline solutions under conditions Standard Bayer. The specific surface of the mechanically activated boehmite is very high, 264 m^2/g, a fact attributed to the shape and density of the pores after structural transformations. It is owing to mechanical stress. The particle size distribution was tracked by the variation in the size of the d90, d50, and d10 classes of the activated material, depending on the activation time, and was presented graphically. According to the data presented, the initial diameter of the particles in these three classes was 153.4, 110.2, and 77.0 μm, respectively. In the first 15 minutes of activation, the characteristic diameters of these classes of particles moved towards small values on the order of hundreds of nanometers. After 240 minutes of activation, the crushing process reverses, and the diameter of the particles increases to the mechanical dimensions of tens of microns. Practically, fine particles resulting from the first phase of mechanical activation agglomerate and form larger particles by extending the activation time. Experimental data presented in the works mentioned above show that the specific BET surface area decreases exponentially by almost 75%, from 264 m^2/g to 67m^2/g, after 240 minutes of mechanical activation.

Other authors also observed the phenomenon during the activation of other minerals, associated with the aggregation of fine particles, when the activation time is prolonged beyond a critical limit [121, 122]. Also, the geometric area of the particles decreases from 2.71 to 2.14 m^2/g as the activation time increases. The decrease in the geometric area of the particles follows the assumption of the aggregation of fine particles in the final stage of activation because some new particles are formed from the activated material and new distributions of particle sizes.

The significant difference between the BET specific surface and the geometric-specific surface attests to the porous nature of the particles formed during mechanical activation. The results demonstrate the change in porosity in the mechanically activated material for shorter or longer activation times. However, the change in porosity type is new evidence of the advanced aggregation of fine particles into particles with new properties acquired in the last activation phase near the activation time of 240 minutes [116, 117].

Before mechanical activation, the XRD data of boehmite display a very clear crystallinity. As far as mechanical activation is extended in time or intensity, the characteristic XRD peaks become increasingly weak. The amorphous is just newly processed material, mostly converted into γ-Al_2O_3 phase at a lower temperature than usual thermal conversion of gibbsite to γ-Al_2O_3.

Mechanical activation of boehmite - boehmite to metastable χ- Al_2O_3 and κ-Al_2O_3

The nanocrystalline boehmite powder (γ-AlOOH) was tested as a precursor for transitions to the χ-Al_2O_3 and κ-Al_2O_3 phases by mechanical activation. A high-energy planetary ball mill was used for this mechanical activation. To the extent that the activation energy was increased, either by grinding

or by increasing the centrifugal force, the boehmite was transformed into χ-Al_2O_3 and κ-Al_2O_3, as metastable phases of alumina. The presence of metastable phases was highlighted by comparison with the X-ray diffraction patterns of the heat-treated gibbsite (γ-$Al(OH)_3$ up to α-alumina). The higher energy transfer to both these phases by milling the material, eventually resulted in the formation of thermodynamically stable α-Al_2O_3. Although boehmite is normally decomposed into γ-Al_2O_3 by heating, phase transformation route of the boehmite is induced by mechanical milling in different way, than it is induced by thermal process. The authors agreed that this change in transition mechanism is due to boehmite crystalline structure over skewed under high mechanical strains [122, 123].

Mechanical activation of boehmite - transition γ Al_2O_3 to α-Al_2O_3

A well-justified combination of phase transitions leads to a technological option for obtaining alumina γ- Al_2O_3, as a precursor of the alpha phase α-Al_2O_3, in the process of mechanical activation of transition γ-Al_2O_3 → α-Al_2O_3. The initial raw material can be the gibbsite and boehmite, in case the crystallinity of the γ Al_2O_3 phase is not of significant importance or the transition γ Al2O3 → α-Al2O3 is done thermally. If the quality of the final α-Al_2O_3 product and energy consumption are priorities, then the synthesis line must be radically changed.

Cortés-Vega et al. found a reasonable solution to produce α-Al_2O_3 of good quality using as the initial precursor, the pseudo-boehmite synthesized by the reaction in an aqueous environment of aluminum sulfate or nitrate with gaseous ammonia [124]. The washed and dried pseudo-boehmite powder is thermally transformed, at a temperature of 300-500ºC, into γ-Al_2O_3. Then the partially agglomerated powder is mechanically activated at room temperature using a SPEX mill. The ground samples had 10 g, and the grinding time varied between 5 and 10 hours. The duration of grinding determines the quality of the ground product. At grinding times shorter than 5 hours, the particles have an irregular shape, which becomes more rounded by increasing the grinding time. In addition to grinding, thermal activation also serves to homogenize the particle sizes of the product.

To avoid contamination, no phase transformation activators were used. Characterization of the finished product (α-Al_2O_3) was characterized by modern XRD and SEM methods. Neither the precursor γ-Al_2O_3 nor the final product (α-Al_2O_3) was contaminated with any specific transition phases accompanying the recrystallization of the substances during thermal activation. This happened because the precursors coming from pure reagents did not contain small seeds of transition phases. The dates collected in this study for α-Al_2O_3, were obtained at ambient temperature and confirmed by other authors [122, 124,125].

Boehmite and pseudo-boehmite as precursors for the manufacture of high-temperature alumina products at low temperatures by mechanical activation

Due to its remarkable hardness and stability, among other strategic applications, alumina (Al_2O_3) can be used in highly corrosive environments, environments with high temperatures, and compressive stresses, as well as for energy storage and harvesting, optical, and photonic applications [126-131]. Naturally occurring alumina is the second hardest material, just a step behind diamond and ruby{α-Al_2O_3-Cr_2O_3(0.2%)}, as a complete solid-state solution (unchanged in both solid and liquid phase) [126,132]. Beyond these avant-garde materials, there are some small domains of application concerning gems and industrial gems. Maybe, due to strict concurrence, it is not many papers available [133-136]. However, the synthesis of such products, assisted by mechanical activation, presents an interesting image of replacing the high-temperature process manufacturing with milling at low temperatures. The α-Al_2O_3-Cr_2O_3 (0.2%) solid solution is commonly known as ruby and bears the substitution of Al^{3+} for Cr^{3+} in octahedral sites [131]. The formation of the solid solution involves a small expansion of the α-Al_2O_3 lattice due to the comparatively larger ionic radius of Cr^{3+} [137].

The ruby is highly sought due to its unique characteristics given by the resonant luminescence bands R1 and R2, which are sensitive to displacement with temperature and pressure. Luminescence bands can be easily detected by Raman spectroscopy. The ruby is in demand as a

precious stone and a sensor with applications in extreme conditions (temperature and pressure). Ruby is synthesized from α-Al_2O_3 (corundum) with additions of Cr^{3+} at temperatures of at least 1200 °C [138-143]. A preliminary thermal approach showed that boehmite mechanically activated undergoes a full dihydroxylation at room temperature. Some changings during further heating were observed at temperatures between 300 and 500°C [144], and the complete transformation to α-Al_2O_3-Cr_2O_3 (0.2%) has taking place during annealing up to 867°C (almost 200°C lower than the conventional transition point).

Actually, in this experiment, the small quantities α-Cr: Al_2O_3 (0.2%) synthesized by mechanical activation at room temperature (first stage) acts as the seed or heterogenous sites for the secondary nucleation process and is responsible for a temperature drop of approximately 200°C (up to 867 °C) for crystallization of the ruby (second stage). The ruby (α-Al_2O_3-Cr_2O_3(0.2%) synthesis at low temperature, via the mechanical activation and via chi-alumina (χ-Al_2O_3) has been made by Cortes-Vega et al. [145, 146] show that the critical problems in this crystal growth synthesis were finding the right concentrations of Cr_2O_3 and using Raman spectroscopy to detect very low concentrations of chromium in ruby-diluted compositions. The presence of (α-Al_2O_3-Cr_2O_3 (0.2%) ruby phase was further confirmed with HRTEM (high-resolution transmission electron microscopy). Also, the microscopy data showed the presence of small crystals of the δ-Al_2O_3 phase.

The analysis of the first experimental results and the more careful study of the crystallographic data of each phase involved in the ruby synthesis showed that the crystallographic parameters of pseudo-boehmite are closer to the ruby crystal structure {α-Al_2O_3-Cr_2O_3 (0.2%)} than the boehmite parameters. Thus, the experiment was repeated with pseudo-boehmite instead of boehmite. The pseudo-boehmite was synthesized by crystallization from an aqueous solution of 0.2 mol/L aluminum sulfate (purity 98% as dried material). The solution was heated to 60 °C and ammoniated under intense stirring up to pH 9-10. The final pH was kept constant over the entire precipitation process. The following reactions are finished at this pH and the pseudo-boehmite is fully precipitated:

$NH_3 + H_2O \rightarrow NH_4^+ + OH^-$

$2Al^{3+} + 3(SO_4)^{2-} + 6(NH_4)^+ + 6(OH)^- \rightarrow 2AlO(OH) + 2H_2O + 3(NH4)_2SO_4$

The obtained crystalline products were filtered and washed with distilled water more times until the washing water showed a constant pH of 7 and ammonium sulfate was completely removed. The resulting product was dried at 100 °C for 24 h. Larger particles were breached in a mortar until the pseudo-boehmite look liked a loose white powder. The raw materials, pseudo-boehmite and Cr_2O_3 have been treated mechano-chemically for the successful synthesis of both χ-Al_2O_3 and ruby {α-Al_2O_3-Cr_2O_3 (0.2%)}. The first pair of samples were prepared with the new precursor. The first sample was mechanically activated by milling for a minimal period necessary to complete the transition from pseudo-boehmite to χ-Al_2O_3. The XRD analysis revealed that the entire quantity of pseudo-boehmite was converted to χ-Al_2O_3.

During the milling process, full dihydroxylation occurs at room temperature, and no traces of other transitional phases were observed accompanying the χ-Al_2O_3. This experiment demonstrated that only mechanical activation makes transition pseudo-boehmite to χ-Al_2O_3 possible at room temperature. Otherwise, this transition is observed during thermal activation at temperatures between 300 and 500 °C [147-150]. The second sample was milled for approximately 30 hours in the SPEX mill. It was found that both transitions pseudo-boehmite to χ-Al_2O_3 and χ-Al_2O_3 to ruby {α-Al_2O_3-Cr_2O_3 (0.2%)} are fully accomplished, in the absence of other Al_2O_3 phases such as θ, γ, κ, and δ. In the milled samples, even in the sample milled for only five hours, the presence of {α-Al_2O_3-Cr_2O_3 (0.2%)} is observed. Due to the very small fractions at the trace level, these were undetectable by the XRD technique. The detection of Cr_2O_3 traces in the synthesized ruby was possible by Raman spectroscopy due to its high sensitivity, capable of detecting even parts per million ruby in a sample [147, 148]. This study demonstrates three significant findings: the room temperature synthesis of χ-Al_2O_3 and α-Cr: Al_2O_3 with SPEX, the changes in phase transformation energy requirements and a 193 °C drop in phase transformation temperature from χ-Al_2O_3 to α-Al_2O_3.

At the same time, in parallel experiments, when the samples were heated, transformation followed the following path: pseudo-boehmite → δ-Al_2O_3 → α-Al_2O_3.
Also, in the milled samples, the transformation path is pseudo-boehmite → χ-Al_2O_3 → α-Al_2O_3, and no presence of γ-Al_2O_3 was observed. Both paths are typically found using pseudo-boehmite as a precursor when the phase transitions are done.
Characterization of the above raw materials, intermediary and final products was carried out utilizing the following types of equipment: a) XRD (X-ray diffraction) using a Siemens D5000 diffractometer with a Bragg–Brentano geometry and Cu-Kα radiation (λ=1.5418 Å); b) Raman spectroscopy using a confocal micro Raman microscope (Xplora™, Horiba JY) and A 532 nm diode laser was used for excitation; c) High-resolution transmission electron microscopy (HRTEM) using a transmission electron microscope (JEM-2200FS JEOL) operated at 200 kV: d) Image analysis for the HRTEM micrographs using Digital Micrograph that is capable of reproducing the fast Fourier transformation (FFT) and their inverse (IFFT) images for a more in-depth analysis. e) Thermal analysis using a SETARAM differential scanning calorimeter (DSC) analyser.

CONCLUSION

This paper completes the row of published research works regarding the low-temperature activated alumina products coming out from the same precursor, the aluminum hydroxide dried, milled, and classified manufactured at Vimetco Alum SA Tulcea, Romania, after implementation of the project "Endow the Research and Development Department of SC ALUM SA Tulcea with independent and efficient research facilities to support the economic competitiveness and business development". The project was co-funded by the European Regional Development Fund through the Competitiveness Operational Program 2014–2020.
The previous papers described the thermal activation principles, laboratory preparation, and characterization of the low-temperature alumina thermal activation products, as well as these products' chemical structure, mineralogy, main properties, and industrial uses.
This paper is a short review of recent research concerning a relatively new technology designed to activate the particular classes of non-metallurgical alumina by mechanical activation at normal environmental temperatures. The main original topics analysed in this paper concerned: Gibbsite mechanical activation. Gibbsite to alfa α-Al_2O_3: Boehmite mechanical activation. Boehmite to alfa α-Al_2O_3: Boehmite mechanical activation. Boehmite to metastable chi χ-Al_2O_3 and kappa κ-Al_2O_3: Boehmite mechanical activation. Transition γ Al_2O_3 to α-Al_2O_3: Boehmite and pseudo-boehmite as precursors for manufacturing high-temperature alumina products at low temperatures by mechanical activation.
Mechanical activation is very used to produce clean alumina mineralogical phases with uniform particle size dimensions from nano to macro size dimension. Also, mechanical activation may extend the specific surface of some minerals, enhancing the yields in the solid-liquid extraction process.
The sustaining literature on the subject matter was selected from published materials in the last years and from fundamental papers published before 2000th.

ACKNOWLEDGMENTS

This study was made possible by the implementation of the *"Endow the Research and Development Department of SC ALUM SA Tulcea with independent and efficient research facilities to support the economic competitiveness and business development"* project, which was co-funded by the European Regional Development Fund through the Competitiveness Operational Program of 2014–2020. Under this project, the following were purchased and commissioned: *"Independent equipment/ installation for research and development of the technology for wet aluminum hydroxide classification"*, *"Independent equipment/installation for research and development of technology for obtaining the dried aluminum hydroxide"*, and *"Independent equipment/installation for research and development of the technology for grinding and screening the dried aluminum hydroxide"*.

REFERENCES

[1] IBRAHIM, I., BAHARUDDIN, S., ARBAIN, R., OTHMAN, A., JOANNES, C., IOP Conf. series: Earth Environ. Sci., **641,** p.1, 2021, https://doi.org/10.1088/1755-1315/641/1/012004.
[2] VASILJEVIC, N., DAMJANOVIC, V., RADISLA, V., FILIPOVIC, R., PERUSIC, M., OBRENOVIC, Z., OLJACA, D., Technol. Acta, **13**, no. 2, 2020, p. 23, http://tf.untz.ba/technologica-acta.
[3] PARK, N.K., CHOI. H.Y., KIM, D.H., LEE, T.J., KANG, M., LEE, V.G., KIM, H.D., PARK, J.W., J. Cryst. Growth, **373**, no. 15, 2013, p. 88, https://doi.org/10.1016/j.jcrysgro.2012.12.004.
[4] DOBRA, G., ILIEV, S., COTET, L., BOIANGIU, A., HULKA, I., KIM, L., CATRINA, G.A., FILIPESCU, L., J. Sib. Fed. Univ. Eng. Technol., **14**, no. 2, 2021, p. 151, http://hdl.handle.net/123456789/1733.
[5] DOBRA, G., GARCIA-GRANDA, S., ILIEV, S., COTET, L., HULKA, I., NEGREA, P., DUTEANU, N., BOIANGIU, A., FILIPESCU, L., Rev. Chim., **71**, no. 9, 2020, p. 65, https://doi.org/10.37358/RC.20.9.8318.
[6] DOBRA, G., ILIEV, S., ANGHELOVICI, N., COTET, L., FILIPESCU, L., Rev. Chim., **70**, 2019, p. 355, https://doi.org/10.37358/RC.19.2.6916.
[7] RIZWAN, M., CHANDAN, M.R., J. Appl. Polym. Sci., **139**, no. 20, 2022, https://doi.org/10.1002/app.52164.
[8] SETYANTO, D., JAYATUN, Y.A., BASOEKI, P.D., DE FRETES, A., Polymers, **14**, 2022, p. 1, https://doi.org/10.3390/polym14122464.
[9] XU, B., LIU, Y., WEI, S., ZHAO, S., QIAN, L., CHEN, Y., SHAN, H., ZHANG, Q., Int. J. Mol. Sci., **23**, no. 19, 2022, https://doi.org/10.3390/ijms231911256.
[10] PIPEROPOULOS, E., SCIONTI, G., ATRIA, M., CALABRESE, L., PROVERBIO, E., Polymers, **14**, no. 3, 2022, p. 1, https://doi.org/10.3390/polym14030372.
[11] VAHIDI, G., BAJWA, D.S., SHOJAEIARANI, J., STARK, N., DARABI, A., J. Appl. Polym. Sci., **138**, no. 12, 2021, p. 1, https://doi.org/10.1002/app.50050.
[12] HARUN-OR-RASHID, G.M., ISLAM, M.M., Int. J. Mater. Sci. Appl., **9**, no. 3, 2020, p. 40, https://doi.org/10.11648/j.ijmsa.20200903.11.
[13] MATYKIEWICZ, D., Materials, **13**, no. 8, 2020, p.1, https://doi.org/10.3390/ma13081802.
[14] ATIQAH, A., ANSARI, M.N.M., KAMAL, M.S.S., JALAR, A., AFEEFAH, N.N., ISMAIL, N., J. Mater. Res. Technol., **9**, no. 6, 2020, p. 12899, https://doi.org/10.1016/j.jmrt.2020.08.116.
[15] RAI, S., CHADDHA, M.J., NIMJE, M.T., KULKARNI, K.J., AGNIHOTRI, A., Res. J. Eng. Technol., **11**, no. 4, 2020, p. 169, https://doi.org/10.5958/2321-581X.2020.00027.6.
[16] HU, S., TAN, Z.W., CHEN, F., LI, J.G., SHEN, Q., HUANG, Z.X., ZHANG, L.M., Fire Mater., **44**, no. 5, 2020, p. 673, https://doi.org/10.1002/fam.2831.
[17] ZHOU, R., MING, Z., HE, J., DING, Y., JIANG, J., Polymers, **12**, no. 1, 2020, p. 1, https://doi.org/10.3390/polym12010180.
[18] KALAV, B., ISMAR, E., KAYAOGLU, B., J. Fac. Eng. Archit., **34**, no. 3, 2019, p. 11, https://doi.org/10.21605/cukurovaummfd.637557.
[19] LI, M., PANG, L., CHEN, M., XIE, J., LIU, Q., Materials, **11**, no. 10, 2018, p. 1, https://doi.org/10.3390/ma11101939.
[20] RAMLI, M.S.A., MISHA, S., HAMINUDIN, B., AFZANIZAM, M., ROSLI, M., YUSOF, A.A., BASAR, M., BIN SOPIAN, K., IBRAHIM, A., FAZLIZAN, A. Int. J. Heat. Technol., **39**, no. 5, 2021, p. 1475, https://doi.org/10.18280/ijht.390509.
[21] MESHCHERYAKOV, E.P., RESHETNIKOV, S.I., SANDU, M.P., KNYAZEV, A.S., KURZINA, I.A., *Appl. Sci.*, **11**, no. 6, 2021, p. 1, https://doi.org/10.3390/app11062457.
[22] MOU, X., CHEN, Z., Ultrason. Sonochem., **70**, 2021, p. 1, https://doi.org/10.1016/j.ultsonch.2020.105314.
[23] MESHCHERYAKOV, E., KOZLOV, M., RESHETNIKOV, S., ISUPOVA, L., LIVANOVA, A., KURZINA, I., *Appl. Sci.*, ***10***, no. 15, 2020, p. 1, https://doi.org/10.3390/app10155320.
[24] ZHANG, H., WANG, Y., ZHANG, Z., NIU, B., J. Phys. Conf. Ser., **1549**, 2020, p. 1, https://doi.org/10.1088/1742-6596/1549/3/032112.

[25] DHULAM, S.D., DADI, M.J., J. Emerg. Technol. Innov. Res., **6**, no. 4, 2019, p. 531, https://www.jetir.org/papers/JETIR1904073.pdf.
[26] Singh, R.P., Mishra, V.K., Das, R.K., IOP Conf. Series: Mater. Sci. Eng., **404**, 2018, p. 1. https://doi.org/10.1088/1757-899X/404/1/012005.
[27] REYES-LOPEZ, S.Y., AGUIRRE-TERRAZAS, K.A., TORRES-PEREZ, J., MEDELLIN-CASTILLO NAHUM. M.C., DE JESUS RUIZ-BALTAZAR, A., Int. J. Res.-Granthaalayah, **9**, no. 4, 2021, p. 435, https://doi.org/10.29121/granthaalayah.9.i4 2021.3846.
[28] ALHASSAN, S.I., HUANG, L., HE, Y., YAN, L., WU, B., WANG, H., Crit. Rev. Environ. Sci. Technol., 2021, 51, no. 18, https://doi.org/10.1080/10643389.2020.1769441.
[29] JASIM., M.A., ABBAS, A.M., RADHI, I.M., AIP Conf. Proceed., 2021, **2372**, no. 1. https://doi.org/10.1063/5.0068746
[30] OSAGIE, C., OTHMANI, A., GHOSH, S., MALLOUM, A., ESFAHANI, Z.K., J. Mater. Res. Technol., **14**, 2021, p. 2195, https://doi.org/10.1016/j.jmrt.2021.07.085.
[31] KIM, J., LEE, H., VO, H.T., LEE, G., KIM, N., JANG, S., JOO, J., BEAD-SHAPED, B., Materials, **13**, no. 6, 2020, p. 1, https://doi.org/10.3390/ma13061375.
[32] KARIMI, Z., ALLAHVERDI, A., OSHANI, F., J. Stud. Color World, **10**, no. 1, 2020, p. 41, DOI: 20.1001.1.22517278.1399.10.2.4.7.
[33] WANG L., SHI C., WANG L., PAN L., ZHANG X., ZOU J., Nanoscale, **12**, 2020, p. 4790, https://doi.org/10.1039/C9NR09274A.
[34] HAMI H. K., ABBAS R. F., ELTAYEF E. M., MAHDIN I., SAMARRA J., Pure Appl. Sci., **2**, no. 2, 2020, p. 19, https://doi.org/10.54153/sjpas.2020.v2i2.109.
[35] CHAIKITTISILP, W., KIM, H.J., JONES, C.V., Energ. Fuel., **25**, no. 11, 2011, p. 5528, https://doi.org/10.1021/ef201224v.
[36] KUMARI, P., ALAM, M., SIDDIQI, W.A., Sustain. Mater. Technol., **22**, 2019, p. 1, https://doi.org/10.1016/j.susmat.2019.e00128.
[37] BANERJEE, S., DUBEY, S., GAUTAM, R.K., CHATTOPADHYAYA, M.C., SHARMA, Y.C., Arab. J. Chem., **12,** no. 8, 2019, p. 5339, https://doi.org/10.1016/j.arabjc.2016.12.016.
[38] OMRANI, M., MALEKMOHAMMAD, M., ZABOLIAN, H., Sci. Rep., **12**, 2022, p. 1, https://doi.org/10.1038/s41598-022-04928-2.
[39] MURALIDHAR SINGH M.M., KUMAR, H., SIVAIAH, P., Int. J. Thin. Fil. Sci. Tec., 2021, **10**, p. 13, https://doi.org/10.18576/ijtfst/100103.
[40] BOUZBIB, M., EL MAROUANI, M., SINKO, K., J. Eur. Opt. Soc.-Rapid Publ., **17**, 2021, p. 1, https://doi.org/10.1186/s41476-021-00170-x.
[41] YANG, X., WANG, G., LIANG, M., YUAN T., RONG, H., Road Mater. Pavement Des., **1**, 2021, https://doi.org/10.1080/14680629.2021.2012239.
[42] MALGAJ, T., MIRT, T., KOCJAN, A., JEVNIKAR, P., Coatings, **11**, 2021, p. 1, https://doi.org/10.3390/coatings11091126.
[43] KUMAR, H., SINGH, M.M., SIVAIAH, P., Int. J. Mater. Eng. Innov., **12**, no. 3, 2021, p. 165, https://doi.org/10.1504/IJMATEI, 2021.116943.
[44] BOUZBIB, M., POGONYI, A., KOLONITS, T., VIDA, A., DANKHAZI, Z., SINKO, K., J. Solgel Sci. Technol., **93**, 2020, p. 262, https://doi.org/10.1007/s10971-019-05193-y.
[45] BASHA, G.M.T., SRIKANTH, A., BOLLEDDU, V., Mater. Today: Proc., 2020, **22**, no. 4, p. 1554, https://doi.org/10.1016/j.matpr.2020.02.117.
[46] INGA, M., FUJII, L., FILHO, J.M.C., PALHARES, J.H.Q., FERLAUTO, A.S., MARQUES, F.C., ALEGRE, T.P.M., WIEDERHECKER. G., APL Photon, **5**, 2020, p. 1, https://doi.org/10.1063/5.0028839.
[47] SPYRA, J., MICHALAK, M., NIEMIEC, A., LATKA, L.A., Sci. Technol. Weld. Join., **92**, no. 4, 2020, p. 17, https://doi.org/10.26628/wtr.v92i4.1107.
[48] ZHANG, H., HONG, Z., JING, G., GUOLONG, L., XUESONG, T., LIGUO, J., J. Polym. Eng., **42**, no. 5, 2022, p. 428, https://doi.org/10.1515/polyeng-2021-0275.
[49] SOURAV, G., RANAJIT, G., HARISH, H., NILRUDRA, M., Ceram. Int., **48**, no. 9, 2022, p. 11879, https://doi.org/10.1016/j.ceramint.2022.02.214.

[50] KRISHNAN, S.V., AMBALAM, M.M., VENKATESA, N.R., MAYANDI, J., VENKATACHALAPATHY, V., Ceram. Int., 2021, **47**, no. 17, p. 23693, https://doi.org/10.1016/j.ceramint.2021.05.146.
[51] IBRAHIM, S.N., ZAIDAN, S.A., MOHAMMED, M.A., AIP Conf. Proceed., **2372**, 2021, p. 1, https://doi.org/10.1063/5.0067304.
[52] HAMMI, M., ZIAT, Y., ZARHRI, Z., LAGHLIMI, C., MOUTCINE, A., Sci. Rep., **11**, 2021, p. 1, https://doi.org/10.1038/s41598-021-91741-y.
[53] GOUDA, K., BHOWMIK, S., DAS, B., Rev. Adv. Mater. Sci., **60**, no. 1, 2021, p. 237, https://doi.org/10.1515/rams-2021-0024.
[54] RAMIREZ, C., BELMONTE, M., MIRANZO, P., OSENDI, M.I., Materials, **14**, no. 9, 2021, p. 1, https://doi.org/10.3390/ma14092111.
[55] KASAR, A.K., MENEZES, P.L., Materials, **13**, no. 20, 2020, p. 1, https://doi.org/10.3390/ma13204502.
[56] COUPAN, R., MOONEN, P., DICHARRY, C., PLANTIER, F., DIAZ, J., PERE, E., KHOUKH, A., ACS Appl. Mater. Interfaces **12**, no. 30, 2020, p. 34137. https://doi.org/10.1021/acsami.0c06187.
[57] GARCIA-BORDEJE, E., DONGIL, A.B., CONESA, J.M., GUERRERO-RUIZ, A., RODRIGUEZ-RAMOS, I., Nanomaterials, 2022, **12**, no. 7, p. 1, https://doi.org/10.3390/nano120710.
[58] JABBARI, A., MORADI, P., HAJJAMI, M., TAHMASBI, B., Sci. Rep., **12**, 2022, p. 1, https://doi.org/10.1038/s41598-022-15921-0.
[59] MOHAMMADI, M., KHODAMORADY, M., TAHMASBI, B., BAHRAMI, K., GHORBANI-CHOGHAMARANI, A., J. Ind. Eng. Chem., **97**, 2021, p. 1. https://doi.org/10.1016/j.jiec.2021.02.001.
[60] FERTAL, D.R., MONAI, M., PROANO, L., BUKHOVKO, M.P., PARK, J., YONG DING, Y., WECKHUYSEN, B.M., BANERJEE, A.C., Catal. Today, **382**, 2021, p. 120, https://doi.org/10.1016/j.cattod.2021.08.005.
[61] RADLIK, M., JUSZCZYK, W., KEMNITZ, E., KARPINSKI, Z., Catalysts 2021, **11**, no. 10, p. 1. https://doi.org/10.3390/catal11101178.
[62] KARAM, L., BACARIZA, M.C., LOPES, J.M., HENRIQUES, C.V., REBOUL, J., EL HASSAN, N., MASSIANI, P., J. CO2 Util., **51**, 2021, p. 1, https://doi.org/10.1016/j.jcou.2021.101651.
[63] PRIECEL, P., KUBICKA, D., VAZQUEZ-ZAVALA, A., ANTONIO DE LOS REYES, J., POUZAR, M., CAPEK, L., Front. Chem., **8**, 2020, p. 1, https://doi.org/10.3389/fchem.2020.00216.
[64] ABASSI, H., Iran. J. Catal., **10**, no. 1, 2020, p. 35, https://www.sid.ir/paper/740217/en#downloadbottom.
[65] KOBRA NIKOOFAR, K., SHAHEDI, Y., CHENARBOO, F.J., Mini-Rev. Org. Chem., **16**, no.2, 2019, p. 102, https://doi.org/10.2174/1570193X15666180529122805.
[66] ABDOLLAHI, J., EMRANI, N., CHAHKANDI, B., MONTAZERI, A., AGHLMAND, R., GHEIBI, M., Ann. Environ. Sci. Toxicol., **5,** no. 1, 2021, p. 59, https://doi.org/10.17352/aest.000038.
[67] WICAKSONO, A.D., AGUSTINA D., MEIDIANA C., IOP Conference Series: Earth Environ. Sci., **940**, 2021, p. 1, https://doi.org/10.1088/1755-1315/940/1/012053.
[68] ISUPOV, V. P., BULINA, N.V., BORODULINA, I. A., Inorg. Mater., **54**, no. 2, 2018, p. 147. https://doi.org/10.1134/S0020168518020073.
[69] OBRADOVIC, N., FAHRENHOLTZ, W.G., FILIPOVIC, S., KOSANOVIC, D., DAPCEVICC, A., DORDEVIC, V.B., BALAC, A., PAVLOVIC, I., Ceram. Int., **45**, no. 9, 2019, p. 1, https://doi.org/10.1016/j.ceramint.2019.03.095.
[70] RAAHAUGE, B.F., WILLIAMS, F.S., Smelter Grade Alumina from Bauxite, Springer Series in Materials Science, US, **320**, 1st ed. 2022, p. 1-15.
[71] LINDSAY, S.J., Light Metals, John Wiley & Sons, US, 2014, p. 597, https://doi.org/10.1007/978-3-319-48144-9_101.

[72] KLETT, C., PERANDER, L., Light Metals, John Wiley & Sons, US, 2015, https://doi.org/10.1002/9781119093435.ch15.
[73] NASIRI, A., ANG, S., J. Electron. Packag., **143**, no. 2, 2021, p. 1, https://doi.org/10.1115/1.4049292.
[74] WU, X., ZHAO, J., SHIMAI, S., MAO, X., ZHANG, J., WANG, S., J. Adv. Ceram., **11**, no. 9, 2022, p. 1375, https://doi.org/10.1007/s40145-022-0615-1.
[75] PARK. Y.Y., LEE, S.O., TRAN, T., KIM, S.J., KIM, M.J., Int. J. Miner. Process., **80**, no. 2, 2006, p. 126, https://doi.org/10.1016/j.minpro.2006.03.006.
[76] LIU, G.H., WANG, P., QI, T.G., LI, H.B., TIAN, X.L., ZHOU, Q.S., PENG, Z.H., Trans. Nonferrous Met. Soc. China, **24**, no. 1, 2014, p. 243, https://doi.org/10.1016/S1003-6326(14)63053-3.
[77] KANG, M.J., YOON, D.H., J. Korean Ceram. Soc., **59**, 2022, p. 595, https://doi.org/10.1007/s43207-022-00192-2.
[78] CHAPLIANKO, S.V., NIKICHANOV, V.V., Sci. Res. Refract. Tech. Ceram., **121**, 2021, p. 103, https://doi.org/10.35857/2663-3566.121.11.
[79] SADIKA, C., EL AMRANIB, I., ALBIZANE, A., J. Asian Ceram. Soc., **2**, 2014, p. 83, https://doi.org/10.1016/j.jascer.2014.03.001.
[80] BERRIN GUREL, S., ALTUN, A., Powder Technol., **196**, no. 2, 2009, p. 115, https://doi.org/10.1016/j.powtec.2009.07.007.
[81] TANG, H., LI, C., GAO, J., TOUZO, B., LIU, C., YUAN, W., Materials, **14**, no. 11, 2021, p. 1, https://doi.org/10.3390/ma14113050.
[82] MA, S., SHIL, K., XIA, Y., Ceram. Int., **46**, no. 7, 2020, p. 1, https://doi.org/10.1016/j.ceramint.2019.12.249.
[83] BELYAEV G. E, GRIGORENKO, A.V., VLASKIN, M.S., LIPATOVA, I.A., SHKOLNIKOV, E.I., ZHUK, A.Z., IOP Publ., J. Phys. Conf. Ser., **1385**, 2019, https://doi.org/.1088/1742-6596/1385/1/012041.
[84] BAGAISKOV, YU., USHAKOV, N., Mater. Res. Proc., **21,** 2022, p. 71, https://doi.org/10.21741/9781644901755-13.
[85] CURTOLO, D.C., XIONG, N., FRIEDRICH, S., FRIEDRICH, B., Metals, **11**, no. 9, 2021, p. 1, https://doi.org/10.3390/met11091407.
[86] SMITH, P., POWER, G., Miner. Process. Extr. Metal. Rev., **43,** no. 6, 2022, p. 747, https://doi.org/10.1080/08827508.2021.1937150.
[87] QINNAN YIN, Q., JIN, H., WU, F., WANG, W., QIAN, Y., IOP Conf. Ser. Earth and Environ. Sci., **898**, 2021, p. 1, https://doi.org/10.1088/1755-1315/898/1/012022.
[88] HART, L. D., ESTHER LENSE, E., Alumina Chemicals: Science and Technology Handbook, Wiley, US, 1990.
[89] Fastmarket, https://www.fastmarkets.com/industrial-minerals/bauxite-alumina.
[90] STEINIKE, U., TKACOVA, K., J. Mater. Synth. Process., **8**, 2000, p. 197, https://doi.org/10.1023/A:1011364110355.
[91] BOLDYREV, V.V., Russ. Chem. Rev., 75, no. 3, 2006, p. 177, https://doi.org/10.1070/RC2006v075n03ABEH001205.
[92] ALEX, T.C., KUMAR, R., SANAT, K., ROY, S.K., MEHROTRA,S.P., Miner. Process. Extr. Metal. Rev., **37**, no. 1, 2016, p. 1, https://doi.org/10.1080/08827508.2015.1055626.
[93] WEFERS, K., MISRA, C., Oxides and Hydroxides of Aluminum, Alcoa Laboratories, Technical Paper No. 19, US, 1987, p.1-100.
[94] KAJDAS, C., Mater. Sci. Appl., **6**, no. 1, 2015, p. 60, https://doi.org/10.4236/msa.2015.61008.
[95] BEYER, M.K., CLAUSEN-SCHAUMANN, H., Chem. Rev., **105**, no. 8, 2005, p. 2291, https://doi.org/10.1021/cr030697h.
[96] ROGACHEV, A.S., Russ. Chem. Rev., **88**, no. 9, 2019, p. 875. https://doi.org/10.1021/cr030697h.
[97] LAPSHIN, O.V., BOLDYREVA, E.V., BOLDYREV, V.V, Russ. J. Inorg. Chem., **66**, no. 3, 2021, p. 433, https://doi.org/10.1134/s0036023621030116.

[98] GRIGORIEVA, T., KORCHAGIN, M., LYAKHOV, N., Kona Powder Part. J., **20**, 2002, p. 144, https://doi.org/10.14356/kona.2002017.
[99] FOURMONT, A., POLITANO, O., LE GALLET, S., DESGRANGES, C., BARAS, F., J. Appl. Phys., **129**, no. 6, 2021, p. 1, https://doi.org/10.1063/5.0037397.
[100] BARRY, T.S., UYSAL, T., BIRINCI, M., MURAT ERDEMOGLU, M., Mining Metall. Explor., **36**, 2019, p. 557, https://doi.org/10.1007/s42461-018-0025-7.
[101] DROZDYUK, T., FROLOVA, M., AYZENSHTADT, A., CALAY, R.K., JHATIAL, A.A., Appl. Sci., **12**, no. 10, 2022, p. 1, https://doi.org/10.3390/app12104957.
[102] PAAVER, P., PAISTE, P., LIIRA, M., KIRSIMAE, K., Minerals, **11**, no. 3, 2021, p. 1, https://doi.org/10.3390/min11010003.
[103] RIVAS MERCURY, J.R.M. SUCUPIRA, M.A., RODRIGUEZ, A.A., CABRAL, A.H., DE AZA, A.H., PENA P., Powder Technol., **362**, 2020, p. 188, https://doi.org/10.1016/j.powtec.2019.11.057.
[104] ALEX, T.C., KUMAR, R., ROY, S.K., MEHROTRA, S.P., Adv. Powder Technol., **19**, no. 5, 2008, p. 483, https://doi.org/10.1016/S0921-8831(08)60914-0.
[105] MEHROTRA, S.P., ALEX, T.C., GREIFZU, G., KUMAR, R., Trans. Indian Inst. Met., **69,** 2016, p. 51 https://doi.org/10.1007/s12666-015-0633-6.
[106] KANO J., MIO H., SAITO F., AIChE J., **46**, no. 8, 2000, p. 1964, https://doi.org/10.1002/aic.690460820.
[107] ALEX, T.C., KUMAR, R., ROY, S.K. MEHROTRA, S.P., Powder Technol., **264**, 2014, p. 105, https://doi.org/10.1016/j.powtec.2014.05.028.
[108] ALEX, T.C. KUMAR, R., ROY, S.K., MEHROTRA, S.P., Powder Technol., **264**, 2014, p. 229, https://doi.org/10.1016/j.powtec.2014.05.029.
[109] YONG, C.C., WANG, J., *J. Am. Ceram. Soc.*, ***84***, *no. 6, 2004, p. 1225*, https://doi.org/10.1111/j.1151-2916. 2001.tb00820.x.
[110] JANG, S. W., LEE, H.Y., SHIN, K.C., LEE, S.M., J. Ceram. Proc. Res., **2**, no. 2, 2001, p. 67.
[111] KARAGEDOV, G. R., Chem. Sustain. Dev., **19,** 2011, p. 339.
[112] KARAGEDOV, G.R., Chem. Sustain. Dev., **26**, 2018, p. 501, https://doi.org/10.15372/CSD20180508.
[113] MACKENZIE, K.J.D., TEMUUJIN, J., OKADA, K., Thermochim. Acta, **327**, 1999, no. 1-2, p. 103, https://doi.org/10.1016/S0040-6031(98)00609-1.
[114] TSUCHIDA, T., ICHIKAWA, N., Reactivity of Solids, 1989, **7**, no. 3, p. 207. https://doi.org/10.1016/0168-7336(89)80037-3.
[115] MUKHAMED'YAROVA, A.N., NESTEROVA, O.V., BORETSKY, K.S., SKIBINA, J.D., BORETSKAYA, A.V., EGOROVA, S.R., LAMBEROV, A.A., Coatings, **9**, no. 1, 2019, p. 1, https://doi.org/10.3390/coatings9010041.
[116] ALEX, T.C., KUMAR, R., ROY, S.K., MEHROTRA, S.P., Powder Technol., **208**, no. 1, 2011, p. 128, https://doi.org/10.1016/j.powtec.2010.12.010.
[117] ALEX, T.C., KUMAR, R., KAILATH, A.J., ROY, S.K., MEHROTRA, S.P., Proceedings of the XI International Seminar on Mineral Processing Technology. Jamshedpur, India, 15-17 December 2010, p. 898, https://eprints.nmlindia.org/2595.
[118] ALEX, T. C., KUMAR, R., ROY, S. K., MEHROTRA, S. P., The fourth Asian Particle Technology Symposium APT, Delhi, India, 14-16 September 2009, p. 284, https://eprints.nmlindia.org/5677.
[119] ALEX, T.C., KUMAR, C.S., KAILATH, A.J., KUMAR, R., ROY, S.K., MEHROTRA, S.P., Metall. Mater. Trans. B, **42**, 2011, p. 592, https://doi.org/10.1007/S11663-011-9494-5.
[120] KARAGEDOV, G.R., LYAKHOV, N.Z., Kona Powder Part. J., **21**, 2003, p. 76, https://doi.org/10.14356/kona.2003011.
[121] Z.Y. Fu, S.L. Wei, Powder Technol., **87**, no. 3, 1996, p. 249, https://doi.org/10.1016/0032-5910(96)03094-X.
[122] DELLISANTI, F. VALDRE G., MONDONICO, M., Appl. Clay Sci., **42**, no. 3, 2009, p. 398. https://doi.org/10.1016/j.clay.2008.04.002.

[123] KOZAWA, T., NAITO, M., Adv. Powder Technol., **27**, no. 3, 2016, p. 935. https://doi.org/10.1016/j.apt.2016.02.025.
[124] CORTES-VEGA, F.D., TORRES P.M., ZARATE-MEDINA, J., Microsc. Microanal., **23**, no. 1, 2017, p. 1644, https://doi.org/10.1017/S1431927617008881.
[125] TONEJC, A., TONEJC, A.M., BAGOVIC, D., Mater. Sci. Eng. A., no. 181–182, 1994, p. 1227.
[126] CHAURUKA, S., HASSANPOUR, A., BRYDSON, R., GHADIRI, M., STITT, E.H., JOHNSON, M., ROBERTS. K.J., Chem. Eng. Sci., **134,** 2015, p. 744, https://doi.org/10.1016/j.ces.2015.06.004.
[127] TRUEBA, M., TRASATTI, S.P., Eur. J. Inorg. Chem., no. 17, 2005, p. 3393, https://doi.org/10.1002/ejic.200500348.
[128] MASUDA, H., ASOH, M., WATANABE, K., NISHIO, M., TAMAMURA, N., Adv. Mater., **13**, no. 3, 2001, p. 189, https://onlinelibrary.wiley.com/doi/10.1002/1521-4095(200102)13:3%3C189 :: AID-ADMA189%3E3.0.CO;2-Z.
[129] KURELLA A. DAHOTRE, N.B., J. Biomater. Appl., **20**, no. 1, 2005, p. 1, https://doi.org/10.1177/0885328205052974.
[130] CHANG, R. H., DOREMUS, L. S., SCHADLER, SIEGEL, R.W., Int. J. Appl. Ceram. Technol., **1**, no. 2, 2005, p. 172, https://doi.org/10.1111/j.1744-7402.2004.tb00167.x.
[131] AZHAR, A.Z.A., CHOONG, L. C., MOHAMED, H., RATNAM M.M., AHMAD Z.A., J. Alloys Compd., **513**, 2012, p. 91, https://doi.org/10.1016/j.jallcom.2011.09.092.
[132] PILLONNET, A., GARAPON, C., CHAMPEAUX, C., BOVIER, C., JAFFREZIC, H., MUGNIER, J., J. Lumin., **87–89**, 2000, p. 1087, https://doi.org/10.1016/S0022-2313(99)00549-9.
[133] EDMONDS, A.M., SOBHAN, M.A., SREENIVASAN, V.K.A., GREBENIK, E.A., RABEAU, J.R., GOLDYS, E.M., ZVYAGIN, V.V., Part. Part. Syst. Charact., **30**, no. 6, 2013, p. 506, https://doi.org/10.1002/ppsc.201200112.
[134] YANG, W., Low temperature synthesis sapphire and ruby and their applications, PhD Thesis 2019, University of Houston, Dept. Mechanical Engineering, USA. https://uh-ir.tdl.org/bitstream/handle/10657/5855/YANG-DISSERTATION-2019.pdf?sequence=1.
[135] BUTCHER, J., Mineral. Mag., **33**, no. 266, 1964, p. 974, https://doi.org/10.1180/MINMAG.1964.033.266.05.
[136] BIN YUAN, B., GUO, Y., LIU, Y., Sci. Rep., **12**, 2022, p. 1, https://doi.org/10.1038/s41598-022-08811-y.
[137] NAZAROVA, A., RADISHEVSKAYA, N., KASATSKY, N., KARAKCHIEVA, N., MATEC Web of Conference, **96**, 2017, p. 1, https://doi.org/10.1051/matecconf/20179600007.
[138] HUANG, J.W., MOOS, H.W., Phys. Rev. J. Archive., **173**, p. 1, 1968, https://doi.org/10.1103/physrev.173.440.
[139] SYASSEN, K., High Press. Res., **28**, no. 2, 2008, p. 75, https://doi.org/10.1080/08957950802235640.
[140] JOVANIC, B.R., Chem. Phys. Lett., **190**, no. 5, 1992, p. 440, https://doi.org/10.1016/0009-2614(92)85169-B.
[141] MAO, H.K., XU J., BELL, P.M., J. Geophys. Res., **91**, no. B5, 1986, p. 4673, https://doi.org/10.1029/JB091iB05p04673.
[142] MA, D.P., ZHENG, X.T., XU, Y.S., ZHANG, Z.G., Phys. Lett. A, **115**, no. 5, 1986, p. 245. https://doi.org/10.1016/0375-9601(86)90475-5.
[143] FUJISHIRO, I., NAKAMURA, Y., KAWASE, T., OKAI, B., JSME, Int. J., Ser. 3, **31**, no. 1, 1988, p. 136, https://doi.org/10.1299/jsmec1988.31.136.
[144] ZHANG Z, R.T. PINNAVAIA, J., Angew. Chem., Int. Ed., **47**, no. 39, 2008, p. 7501, https://doi.org/10.1002/anie.200802278.
[145] CORTES-VEGA, F.D., WENLI, Y., ZARATE-MEDINA, J., BRANKOVIC, S.R., HERRERA RAMÍREZ, J.M.., ROBLES HERNANDEZ, F.C., Cryst. Eng. Comm., **20**, no. 25, 2018, p. 3505, https://doi.org/10.1039/C8CE00360B.

[146] CORTES-VEGA, F.D., WENLI, Y., ZARATE-MEDINA, J., BRANKOVIC, S.R., CALDERON, H.A., ROBLES HERNANDEZ, F.C., J. Am. Ceram. Soc., **102**, no. 3, 2019, p. 976, https://doi.org/10.1111/jace.16171.
[147] ZHANG, S. KHOR K.A. LU, L., J. Mater. Process. Technol., **48**, no. 1-4, 1995, p. 779, https://doi.org/10.1016/0924-0136(95)91416-Z.
[148] CALDERON, H.A., ESTRADA-GUEL, I., ALVAREZ-RAMÍREZ, F., HADJIEV, V.G. ROBLES HERNANDEZ F.C., Microsc. Microanal., **22**, no. 3, 2016, p. 1250. https://doi.org/10.1017/S1431927616007091.
[149] GILMAN, P.S., BENJAMIN J.S., Annu. Rev. Mater. Sci., **13**, 1983, p. 279, https://doi.org/10.1146/annurev.ms.13.080183.001431.
[150] SURYANARAYANA, C., Prog. Mater. Sci., **46**, 2001, no. 1-2, p. 1, https://doi.org/10.1016/S0079-6425(99)00010-9.

Citation: Kim, L., Dobra, G., Isopescu, R., Iliev, S., Cotet, L., Boiangiu, A., Filipescu, L., Short review on mechanical activation in non-metallurgical alumina production, *Rom. J. Ecol. Environ. Chem*., **2022**, 4, no. 2, pp. 62-79.